Eleventh International Conference on CFD in the Minerals and Process Industries
CSIRO, Melbourne, Australia
7-9 December 2015

TRANSIENT SIMULATION OF ACCUMULATING PARTICLE DEPOSITION ON A CYLINDER IN CROSS-FLOW

James N. HEWETT[1*] and Mathieu SELLIER[1]

[1] Department of Mechanical Engineering, University of Canterbury, Christchurch 8140, NEW ZEALAND
*Corresponding author, E-mail address: james@hewett.nz

ABSTRACT

Fouling in pipe systems, including heat exchangers, is an expensive problem in geothermal and oil & gas industries. This study investigates the temporal accumulation of fouling material in piping systems using numerical simulations.

The local rate of particle deposition is influenced by the interaction between the surrounding fluid and wall surface geometry. Therefore, this coupling of the fluid-wall interaction is a key component of the CFD model. This criterion requires an evolving solid deposition region that develops through time and is a function of the particle wall flux.

This study explores the accumulating deposition profile of fouled material on a cylinder in cross-flow through time; representing flow over pipes in heat exchangers. Comparisons are drawn between our numerical simulations and those found in experiments.

Keywords: deposition, multiphase, particle, colloid, silica, scaling.

NOMENCLATURE

Latin Symbols

D	Cylinder diameter, [m].
C_C	Cunningham correction factor.
C_d	Drag coefficient.
C_l	Lift coefficient.
$C_{p,b}$	Pressure coefficient at the base of the cylinder.
d	Particle diameter, [m].
F	Force, [N].
$\mathbf{g}$	Gravity, [m/s^2].
k_B	Boltzmann constant, [J/K].
L_r	Recirculation length, [m].
N	Number of particles.
p	Pressure, [Pa].
St	Strouhal number.
T	Temperature, [K].
t	Time, [s].
$\mathbf{u}$	Velocity, [m/s].
U_∞	Freestream velocity, [m/s].

Greek Symbols

η	Particle capture efficiency.
θ	Angle from the stagnation point, [^{o}].
λ_2	Lambda-2 criterion.
μ	Dynamic viscosity, [kg/m.s].
ζ	Gaussian random number.
ρ	Density, [kg/m^3].

Subscripts

B	Brownian.
dep	Deposited particles.
d	Drag.
f	Continuous (fluid) phase.
i	Index *i*.
p	Discrete (particle) phase.
sep	First separation point.

INTRODUCTION

Silica scaling in pipe systems, including heat exchangers, is an expensive problem in the geothermal industry. The deposited material accumulates on pipe surfaces and adversely affects the thermal conductivity of heat exchangers and reduces the effective cross section of pipes which may lead to clogging (Brown and Dunstall 2000). A similar problem is faced in the oil & gas industry with calcium carbonate scaling (Zhang et al. 2001).

Water in geothermal reservoirs at high temperature and pressure is in chemical equilibrium with the surrounding rock. The temperature and pressure of this water decreases as it is extracted from the reservoir and cycled through the pipe systems. Silica concentration then exceeds the amorphous silica solubility leading to precipitation. These colloidal silica particles are transported to pipe surfaces and gradually accumulate.

Particle deposition on solid walls has been widely studied for aerosols (Fan and Ahmadi 1995, Guha 1997, Tian and Ahmadi 2007, Guha 2008, Mehel et al. 2010) and to a lesser extent for hydrosols (Dupuy et al. 2014). Aerosols have a high particle to fluid density ratio (around 10^3 for gas-particle flows) whereas hydrosols have a low particle to fluid density ratio (around unity for liquid-particle flows).

Particles deposit only when they are both transported to a surface and are then captured by this surface. In this paper, we assume all particles that are transported to the surface are captured. However, only a small portion of silica particles which encounter a wall actually deposit; this chance is termed the attachment probability (Kokhanenko et al. 2014). This assumption is reasonable for our study because we are interested in the development of the deposit morphology rather than the quantitative deposition rate.

Particle-laden flows have been studied in a range of geometries including cylinder in cross-flow (Haugen and Kragset 2010). However, most studies of particle

Copyright © 2015 CSIRO Australia

deposition on cylinder in cross-flow have particle diameters on the order of 100 μm (Palmer et al. 2004) and greater (Krick and Ackerman 2015). Our study of colloidal silica particles have particle diameters ranging from 25 nm to 125 nm (Dunstall et al. 2000).

Several particle capture mechanisms exist: direct interception, gravitational deposition, inertial impaction and diffusional deposition (Spielman 1977). The former three mechanisms are significant for particles that are buoyant (with high particle to fluid density ratio) and large (diameters greater than around 1 μm). Our study investigates non-buoyant, colloidal particles (submicron diameters) which are primarily transported by Brownian and turbulent diffusion.

The Euler-Lagrange approach is commonly used for simulating particle-laden flows; particles are tracked in the Lagrangian reference frame and the surrounding fluid is modelled in the Eulerian reference frame. Particle trajectories are solved based on Newton's second law, including drag, gravity and Brownian diffusion terms.

The gradual accumulation of silica particles on the cylinder wall affects the effective surface. This non-uniform change in deposit morphology over time affects the surrounding fluid flow. One approach of simulating this temporal deposition and the effect on the fluid flow is to simulate the deposited particles with four-way coupling using a soft-sphere model. However, this approach is computationally expensive for many particles because of the extensive coupling between particle-particle interactions; but this strategy has been successful for sedimenting particles in turbulent pipe flow in the context of dune formation (Arolla and Desjardins 2015). Another more tractable approach is to remove particles from the domain when deposited and convert fluid cells to solid cells once they become effectively blocked. This method of modelling fouling evolution has been developed and used for diesel engine exhaust gas systems (Paz et al. 2013).

We have simulated particle deposition of silica colloids on a cylinder in cross-flow. Our findings are compared with two experiments in literature (Dunstall et al. 2000, Garibaldi 1980) where silica scaling is measured on cylinders and flat plates in cross-flow over a period of several weeks. To model the accumulating deposit layer, we employed a similar fouling evolution model to Paz et al. (2013). However, our contribution was that instead of using a semi-empirical relation for the deposition, the particle trajectories were directly solved with a Lagrangian approach.

MODEL DESCRIPTION

Geometry and Mesh

Both sets of experiments (Brown and Dunstall 2000, Garibaldi 1980) observed the deposition of silica particles on a cylinder in cross-flow. The cylinders were placed within a surrounding pipe or channel. However, care was taken to ensure the tunnel test section did not significantly affect the flow by using a 16 % tunnel blockage ratio (Dunstall et al. 2000).

The computational domain was bounded by a large exterior circular cylinder and a small interior circular cylinder which represented the pipe surface. A pipe diameter of D = 25 mm was selected to compare directly with Brown and Dunstall (2000), a similar pipe diameter of 38 mm was used by Garibaldi (1980).

An O-type structured mesh was used with 200 circumferential by 110 radial cells in the cross-sectional plane and 1 (2-D) or 32 (3-D) cells in the spanwise direction; which gave 22,000 (2-D) and 704,000 (3-D) cells. The computational domain had a length of πD and a radial extension of 5D. The domain dimensions and grid resolution were based on, and then results verified against, literature including simulations and experiments (Lysenko et al. 2012).

The control volumes (CV) were clustered near the cylinder (Figure 1) to capture the near-wall effects while coarser CV were used further afield in the freestream to optimise computation time without sacrificing accuracy in the near-wall region. The near-wall region (where the fluid cells could switch to solid cells) had a constant radial size (125 μm) to ensure a constant first cell height throughout the simulation.

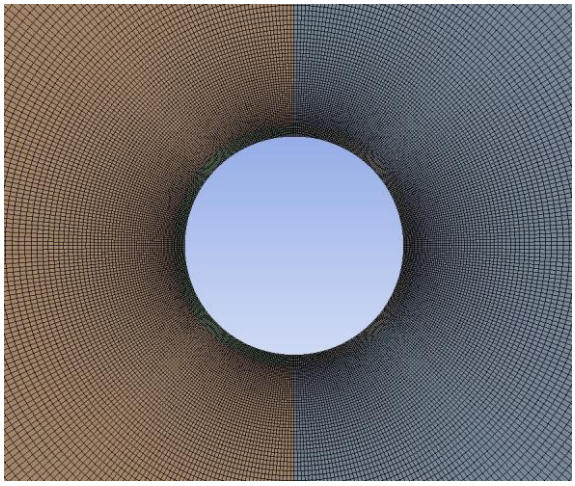

Figure 1: Close-up of mesh near the cylinder.

Continuous Phase

The Navier-Stokes equations were solved for the transient, isothermal simulations using the finite volume method with the commercial CFD package ANSYS Fluent 15.0. The continuity and momentum equations for the continuous phase are:

$$\frac{\partial \rho_f}{\partial t} + \nabla \cdot \left(\rho_f \mathbf{u}_f \right) = 0 \qquad (1)$$

$$\frac{\partial \rho_f \mathbf{u}_f}{\partial t} + \nabla \cdot \left(\rho_f \mathbf{u}_f \mathbf{u}_f \right) = -\nabla p + \nabla \cdot \mu \nabla \mathbf{u}_f \qquad (2)$$

Turbulence was modelled using the Large Eddy Simulation (LES) model with the Smagorinsky-Lilly subgrid-scale model. The pressure-based solver with PISO was used for the pressure-velocity coupling. Spatial discretisation for the pressure used the standard solver and momentum used bounded central differencing. A non-iterative time advancement method was employed for the transient discretisation with a bounded second order

Copyright © 2015 CSIRO Australia

implicit method. These settings were based on a guide from Menter (2012) for simulating scale-resolving flows. Our run times were significantly lower than others (Young and Ooi 2007) who used a different transient method: our simulations required 7.5 hours run time (Intel i7-2600) compared to their 147 hours run time (8 CPUs) for 30 shedding periods in the 3-D LES case. The processor we used was several generations newer, however, the speedup was significantly greater than the difference in hardware.

A Reynolds number, based on D, of approximately 107,000 was used in the experiment which is in the subcritical ($300 < Re < 300{,}000$) flow regime for cylinder in cross-flow (Sumer and Fredsøe 2006). This regime experiences a completely turbulent wake, and laminar boundary layer separation near the top and bottom of the cylinder. We used a Reynolds number in the same subcritical flow regime of Re = 3900 to reduce computational time without compromising the qualitative features of the flow. The fluid was water with a density $\rho_f = 1{,}000$ kg/m^3.

Discrete Phase

The particles had a uniform diameter of d_p = 125 nm and density $\rho_p = 1500$ kg/m^3. The discrete phase was modelled with ANSYS Fluent's Discrete Phase Model (DPM) using the Lagrangian approach. Particles were treated with unsteady particle tracking and were solved simultaneously with the transient fluid simulations. Post-processing of particle depositions was performed with MATLAB.

Particle trajectories were predicted by equating their inertia with forces acting on the particles:

$$\frac{d\mathbf{u}_p}{dt} = F_d\left(\mathbf{u}_f - \mathbf{u}_p\right) + \frac{\mathbf{g}(\rho_p - \rho_f)}{\rho_p} + \mathbf{F}_B \qquad (3)$$

The Stokes-Cunningham drag law, appropriate for submicron particles, was employed ($C_C \approx 1$ for hydrosols):

$$F_d = \frac{18\mu}{{d_p}^2 \rho_p C_C} \qquad (4)$$

Brownian diffusion was modelled with a Gaussian white noise process (Li and Ahmadi 1992) for each particle per time step in all spatial directions:

$$F_{Bi} = \zeta_i \sqrt{\frac{216\mu k_B T}{\pi {d_p}^5 {\rho_p}^2 C_C \Delta t}} \qquad (5)$$

where ζ_i is a zero-mean, unit-variance-independent Gaussian random number.

One-way coupling between the two phases was accounted for where only the particles were influenced by the surrounding fluid. The particle effects on the flow and particle-particle interactions were not taken into account. This assumption is valid for dilute particle concentrations where the particle volume fraction is less than 10^{-6} (Jakobsen 2014).

Particles were injected upstream of the cylinder at a normal distance of 2D from the cylinder axis. This distance was adequately upstream to avoid the near-wall effects of the cylinder. Particles were randomly placed, with a uniform distribution, in an area the size of the cylinder: πD parallel to the cylinder axis and D normal to the cylinder axis and flow. Particles were also randomly distributed in the flow direction, across a space of $U_\infty \Delta t$, to avoid time-dependent patches of particle deposition.

A number of particles, N_p = 1000, were injected every time step. The particles either escaped at the outlet or were captured by the cylinder and removed from the simulation. A total of approximately 300,000 particles were simulated at each time step when the simulation was fully developed for both the continuous and discrete phases. Particle deposition results were recorded after both phases were fully developed. Deposition profiles were evaluated over a period of time which was a multiple of the vortex period to avoid bias due to vortex cycles.

Boundary Conditions

The velocity inlet (located on the left end of the domain) boundary condition was treated as laminar with a freestream velocity of $\mathbf{u} = U_\infty \hat{\mathbf{i}}$ where U_∞ = 0.157 m/s. Turbulent perturbations were not added at the inlet because of the large CV used at the inlet and thus these perturbations would be highly damped and not affect the flow near the cylinder (Breuer 1998). These inlet conditions were used as the initial conditions which resembled a cylinder instantly stopping within the fluid flow from an initial freestream velocity.

A pressure outlet boundary condition was used at the outlet (located on the right end of the domain). The boundary layer was resolved by the mesh in the near-wall region. A no-slip shear condition was used on the cylinder wall and all particles that encountered the wall were assumed deposited (100 % attachment probability). Periodic boundary conditions were used on the ends of the cylinder to allow vortices to develop in the span-wise direction.

Block Mesh Method for Accumulating Deposition

The gradual accumulation of deposited particles was represented by solid sections of the mesh on a cell-by-cell basis. A fluid cell was converted to a solid cell after a number of particles had deposited on the adjacent wall, N_{dep}, such that their volume fraction exceeded the volume of this cell. This irreversible process is shown in Figure 2 and is similar to the general approach employed by Paz et al. (2013).

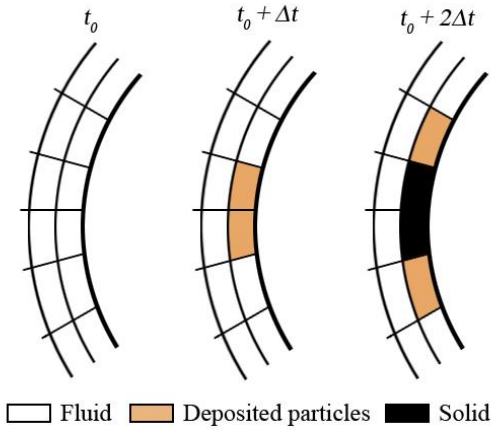

Figure 2: Scheme of the accumulation of deposited material.

Copyright © 2015 CSIRO Australia

The block mesh method assumes that the deposited particles completely block, by volume fraction, the respective mesh cell. However, the agglomerates of particles and the deposition form a porous structure. The volume fraction of the porous medium would be an important consideration for the effective thermal resistance in heat exchangers due to fouling. We assume the porosity of the deposition, on a micrometre scale, has negligible effects on the hydrodynamics.

For every deposited particle: (1) the particle reached the cylinder surface, (2) final particle positions and other details were saved to a data file, and (3) incremented N_{dep} of the cell where the particle resided in (stored with User-Defined Memory). At the end of each time step cells were marked for switching cell type if $N_{dep} \geq 10$. Lastly, every few time steps the marked cells were changed from type fluid to solid.

This procedure was applied in ANSYS Fluent with the use of both User-Defined Functions (UDFs) and Scheme scripts. The UDFs were parallelised and all simulations were performed in parallel mode on a standard desktop computer.

The local fouling evolution of the deposited particles, resulting in a deposition profile, was our primary interest. The particle deposition flux, commonly referred to in terms of the dimensionless deposition velocity, was not a key objective and therefore an arbitrary, single particle was included in each parcel of the DPM. N_{dep} = 10 was chosen because a greater N_{dep} did not significantly alter the morphology of the deposition and had acceptable computational costs.

The cell changes were allowed only after every five time steps to ensure the fluid retained acceptable residuals between changes. There were typically a couple of cell changes at each update; too many changes in one time step caused convergence issues.

RESULTS

Flow Over a Cylinder in Cross-Flow

To accurately predict the deposition of colloidal particles on a cylinder in cross-flow, the surrounding fluid phase must also be accurate. LES was used as the turbulence model and both 2-D (1 spanwise cell) and 3-D (32 spanwise cells) simulations were run and compared with literature. A time step of Δt = 5 ms was used and average fluid statistics were based on more than 50 vortex periods.

Figure 3 shows the vortex shedding phenomenon and the transition between the laminar flow upstream towards the turbulent flow downstream in the wake of the cylinder. The turbulent structures are small in the wake of the cylinder and become larger further downstream. The mesh was concentrated near the cylinder to capture the high velocity gradients influencing the discrete phase due to the near-wall effects.

Turbulent flow over a cylinder in the subcritical flow regime is a common benchmark case; both experimental and LES results are available in the literature for validation. The unsteady, oscillating near wake of the circular cylinder has been quantitatively measured with hot-wire anemometry (HWA) and particle image velocimetry (PIV) experiments in the past. Our 3-D LES runs compare favourably with experiments and previous LES studies as shown in Table 1. The 2-D LES case was used for the particle deposition simulations because of the computational constraint with the evolving mesh. However, the 2-D case yielded a similar vortex shedding frequency and general flow features of the cylinder in cross-flow.

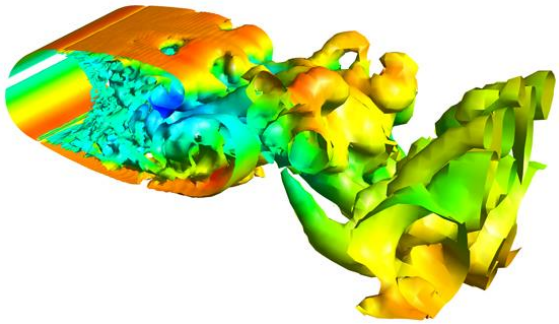

Figure 3: Isosurfaces of λ_2 for the flow over a cylinder at Re = 3900 (coloured by streamwise velocity).

Particle Deposition on a Smooth Cylinder

The colloidal silica particles generally followed the streamlines of the surrounding fluid around the cylinder. The primary transport mechanism for the particles to reach the cylinder surface was Brownian diffusion. Gravity had a negligible effect on the deposition in both our results and from experiments (Brown and Dunstall 2000); the axis of the vertical cylinder axis was aligned with gravity. Some particles were trapped within the flow vortices and had long residence times as shown in Figure 4.

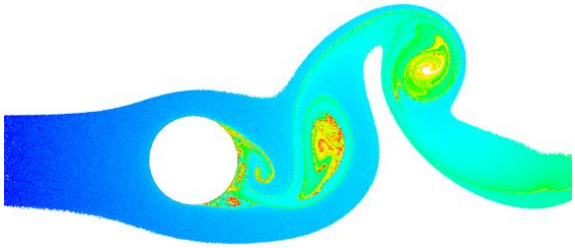

Figure 4: Colloidal particles around a cylinder at Re = 3900 (coloured by particle residence time).

The deposition profile, shown in Figure 5, has similar characteristics to the experimental profile from Garibaldi (1980), shown in Figure 6, specifically: greatest deposition was found at the stagnation point and a smaller peak of deposit was found at θ = 150°. However, they observed deposition between these peaks (to a lesser

Cases	Method	$\langle C_d \rangle$	$(C_l)_{rms}$	St	$-\langle C_{p,b} \rangle$	$\langle L_r \rangle / D$	$-\langle u_{min} \rangle / U_\infty$	$\langle \theta_{sep} \rangle$
Experiments†	HWA, PIV	0.98 – 0.99	0.04 – 0.15	0.20 – 0.22	0.90	1.19 – 1.51	0.24 – 0.34	86
Lysenko et al. (2012) ‡	LES (3-D)	0.97	0.09	0.209	0.91	1.67	0.27	88
Present	LES (2-D)	1.44	1.08	0.23	1.55	0.66	-0.01	111
	LES (3-D)	1.14	0.20	0.22	0.91	1.35	0.28	90

Table 1: Parameters and integral flow features of a cylinder in cross-flow at Re = 3900 compared to literature. †Values are taken from a range of experiments listed by Lysenko et al. (2012). ‡Mach number = 0.2.

Copyright © 2015 CSIRO Australia

extent) covering the cylinder whereas our simulations indicated no deposition within 30° and 130° from the stagnation point.

We assumed a laminar inlet flow condition whereas the cylinders were enclosed within pipes and channels in the experiments causing turbulent conditions upstream. This enhanced turbulence mixing for the particles could explain the greater coverage of deposition in the experiments.

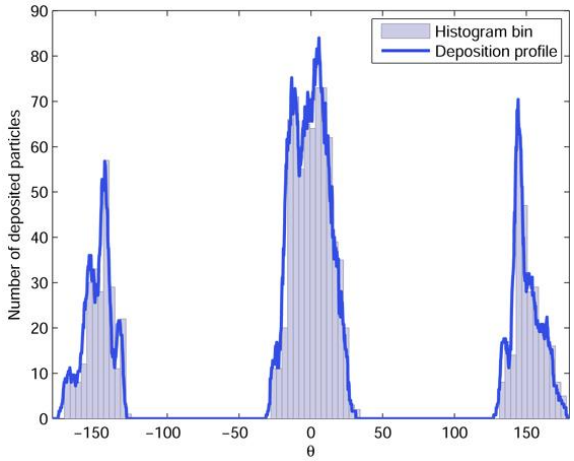

Figure 5: Colloidal particle deposition on a smooth cylinder in the subcritical flow regime over six vortex shedding cycles and with 846,000 injected particles.

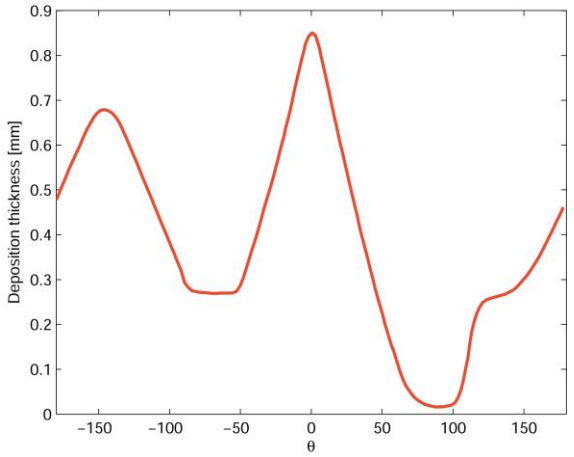

Figure 6: Profile of the scale layer thickness around a cylinder in cross-flow experiment (Garibaldi, 1980).

Capture of particles on a cylinder is often described by the capture efficiency, η, which is the ratio between the deposited and injected particles spanning the cylinder diameter upstream. A η = 0.14 % was found for our smooth cylinder case, and this value agrees well with general trends and extrapolation from experiments (Palmer et al. 2004).

The mass flux of silica deposition on the cylinder was 332 mg/cm^2.day which is significantly higher than the experimental value of 2.52 mg/cm^2.day (Garibaldi, 1980). This mass flux is dependent on η and the mass flow rate of silica in the flow (where the silica content was 549 ppm). Particle reflection (less than 100 % sticking probability) and resuspension are two mechanisms which could explain the higher deposition rate in our simulations when compared with the experiment.

Accumulating Particle Deposition Profile

The accumulation of particles resulted in solid cells which affected the velocity field around the cylinder. Regions of near stagnant flow were produced between peaks of deposits. Particles rarely diffused through these regions, as shown in Figure 7, and instead were transported along streamlines.

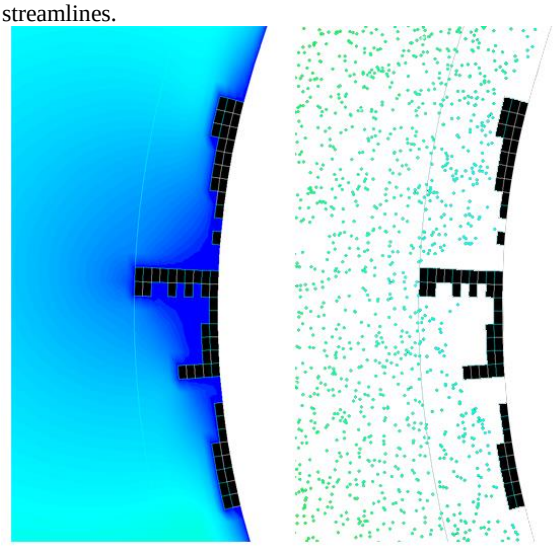

Figure 7: Contours of velocity magnitude (left) and particle positions (right) near the stagnation point around an evolving cylinder wall in the subcritical flow regime.

Local peaks of deposit, shown as black cells in Figure 7, were present in our results near the stagnation point. Both experiments found similar features including needle-like, fibrous structures (Garibaldi 1980) and picket fences (Brown and Dunstall 2000) aligned with the cylinder axis. The size of these peaks in our model was restricted by the mesh resolution which was constrained by computational resources. The fibrous structures (Garibaldi 1980) were on a smaller scale than our mesh but we qualitatively produced this phenomenon in our simulations.

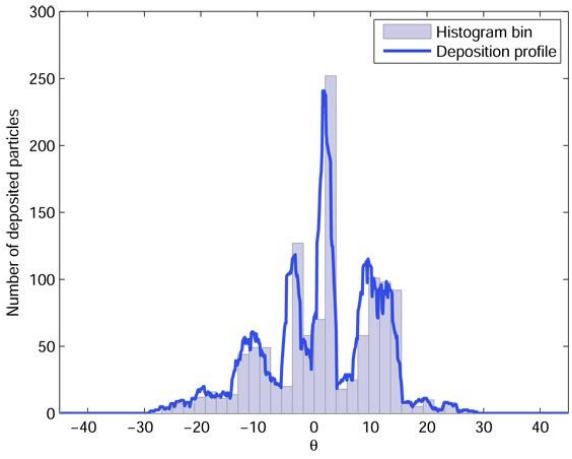

Figure 8: Colloidal particle deposition on an evolving cylinder wall near the stagnation point in the subcritical flow regime over ten vortex shedding cycles and with 1.44 million injected particles.

Copyright © 2015 CSIRO Australia

A similar capture efficiency of η = 0.14 % was also found for the accumulating deposit case compared with the smooth cylinder. However, the particle deposition was concentrated at the peaks around θ = ±3° and ±10°, as shown in Figure 8. Fewer particles reached the cylinder surface after the peaks formed because their transport mechanism was only Brownian diffusion in these near stagnant regions of flow.

CONCLUSIONS

Transient simulations of colloidal particles towards a cylinder in cross-flow in the subcritical flow regime were studied using the DPM and LES with ANSYS Fluent. The gradual accumulation of silica on the cylinder wall was modelled with an evolving mesh where fluid cells were switched to solid cells after a number of particles deposited onto the neighbouring cylinder surface.

The main conclusions are:
(1) Colloidal particles generally follow the streamlines of the surrounding fluid which resulted in low capture efficiencies of 0.14 %. The major transport mechanism responsible for particles to deviate from streamlines and deposit is Brownian diffusion. Gravity has negligible effects on the deposition of small, colloidal particles.
(2) Our deposition profile had reasonably good agreement with an experiment where deposition peaked at the stagnation point and to a lesser extent near the base of the cylinder. However, we found no deposition between these two peaks unlike the experiment. This discrepancy could be because we assumed laminar inflow conditions whereas the experiment had turbulent flow upstream of the cylinder. Furthermore, surface charge interactions between the silica colloids and the steel cylinder surface were not accounted for in our model.
(3) The accumulated deposit formed local peaks on the cylinder surface near the stagnation point, aligned with the axis of the cylinder. Particles were less inclined to deposit on the cylinder surface between peaks because they were only transported by Brownian diffusion within these near stagnate flow regions. Our relatively large deposit peaks had similar characteristics to the fibrous structures found in experimental work.

Fouling of particulate matter is an issue in both the geothermal (silica scaling in heat exchangers and reinjection wells) and oil & gas (calcium carbonate scaling) industries. By improving our understanding of particle deposition we can more accurately predict the rate of fouling and design engineering systems accordingly. Our model could be run in 3-D to predict the 3-D structures on the leeward side of the cylinder. Future work could apply our model to turbulent flow within a pipe.

REFERENCES

AROLLA, S. K., and DESJARDINS, O. (2015), "Transport modeling of sedimenting particles in a turbulent pipe flow using Euler–Lagrange large eddy simulation", *International Journal of Multiphase Flow*, **75**, 1-11.

BREUER, M. (1998), "Large eddy simulation of the subcritical flow past a circular cylinder: Numerical and modeling aspects", *International Journal for Numerical Methods in Fluids*, **28**(9), 1281-1302.

BROWN, K., and DUNSTALL, M. (2000), "Silica scaling under controlled hydrodynamic conditions", *Proceedings World Geothermal Congress*, Kyushu-Tokohu, Japan.

DUNSTALL, M., ZIPFEL, H., and BROWN, K. (2000), "The onset of silica scaling around circular cylinders", *Proceedings World Geothermal Congress*, Kyushu-Tokohu, Japan.

DUPUY, M., XAYASENH, A., WAZ, E., LE BRUN, P. and DUVAL, H., (2014), "Analysis of particle deposition from turbulent liquid-flow onto smooth channel walls", *10th International Conference on CFD in Oil & Gas, Metallurgical and Process Industries*, SINTEF, Trondheim, Norway.

FAN, F., and AHMADI, G. (1995), "Analysis of particle motion in the near-wall shear layer vortices— application to the turbulent deposition process", *Journal of Colloid and Interface Science*, **172**(2), 263-277.

GARIBALDI, F. (1980), "The effect of some hydrodynamic parameters on silica deposition", *Diploma Project 80.11*, Geothermal Institute, University of Auckland.

GUHA, A. (1997), "A unified Eulerian theory of turbulent deposition to smooth and rough surfaces", *Journal of Aerosol Science*, **28**(8), 1517-1537.

GUHA, A. (2008), "Transport and deposition of particles in turbulent and laminar flow", *Annual Review of Fluid Mechanics*, **40**(1), 311-341.

HAUGEN, N. E. L., and KRAGSET, S. (2010), "Particle impaction on a cylinder in a crossflow as function of stokes and Reynolds numbers", *Journal of Fluid Mechanics*, **661**, 239-261.

JAKOBSEN, H. A. (2014), "*Chemical Reactor Modelling: Multiphase Reactive Flows*", Springer, Switzerland.

KRICK, J., and ACKERMAN, J. D. (2015), "Adding ecology to particle capture models: Numerical simulations of capture on a moving cylinder in crossflow", *Journal of Theoretical Biology*, **368**, 13-26.

KOKHANENKO, P., BROWN, K., and JERMY, M. (2014), "Hydro-and electrochemical aspects of silica colloid deposition from a turbulent flow onto a rough wall", *19th Australasian Fluid Mechanics Conference*, Melbourne, Australia.

LI, A., and AHMADI, G. (1992), "Dispersion and deposition of spherical particles from point sources in a turbulent channel flow", *Aerosol Science and Technology*, **16**(4), 209-226.

LYSENKO, D. A., ERTESVÅG, I. S., and RIAN, K. E. (2012), "Large-eddy simulation of the flow over a circular cylinder at Reynolds number 3900 using the OpenFOAM toolbox", *Flow, Turbulence and Combustion*, **89**(4), 491-518.

MEHEL, A., TANIÈRE, A., OESTERLÉ, B., and FONTAINE, J. (2010), "The influence of an anisotropic Langevin dispersion model on the prediction of micro- and nanoparticle deposition in wall-bounded turbulent flows", *Journal of Aerosol Science*, **41**(8), 729-744.

MENTER, F. R. (2012), "Best practice: scale-resolving simulations in ANSYS CFD", ANSYS Germany GmbH.

PALMER, M. R., NEPF, H. M., PETTERSSON, T. J. R., and ACKERMAN, J. D. (2004), "Observations of particle capture on a cylindrical collector: Implications for particle accumulation and removal in aquatic systems", *Limnology and Oceanography*, **49**(1), 76-85.

Copyright © 2015 CSIRO Australia

PAZ, C., SUÁREZ, E., EIRÍS, A., and PORTEIRO, J. (2013), "Development of a predictive CFD fouling model for diesel engine exhaust gas systems", *Heat Transfer Engineering*, **34**(8-9), 674.

SPIELMAN, L. A. (1977), "Particle capture from low-speed laminar flows", *Annual Review of Fluid Mechanics*, **9**(1), 297-319.

SUMER, B. M., and FREDSØE, J. (2006), "*Hydrodynamics around cylindrical structures*" (Rev. ed.). London; Singapore: World Scientific Pub.

TIAN, L., and AHMADI, G. (2007), "Particle deposition in turbulent duct flows—comparisons of different model predictions", *Journal of Aerosol Science*, **38**(4), 377-397.

YOUNG, M. E., and OOI, A. (2007), "Comparative Assessment of LES and URANS for Flow Over a Cylinder at a Reynolds Number of 3900", *16th Australasian Fluid Mechanics Conference*, Gold Coast, Australia.

ZHANG, Y., SHAW, H., FARQUHAR, R., and DAWE, R. (2001), "The kinetics of carbonate scaling—application for the prediction of downhole carbonate scaling", *Journal of Petroleum Science and Engineering*, **29**(2), 85-95.

Copyright © 2015 CSIRO Australia